Neurobiology of Pain 12 (2022) 100104

Contents lists available at ScienceDirect

Neurobiology of Pain

journal homepage: www.sciencedirect.com/journal/neurobiology-of-pain

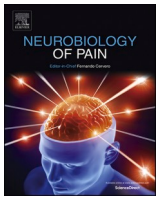

Original Research

Anandamide in the dorsal periaqueductal gray inhibits sensory input without a correlation to sympathoexcitation

Christopher J. Roberts [a,b], Francis A. Hopp [b], Quinn H. Hogan [a,b], Caron Dean [a,b,*]

[a] Department of Anesthesiology, Medical College of Wisconsin, Milwaukee, WI 53226, USA
[b] Department of Anesthesiology, Zablocki Veterans Affairs Medical Center, Milwaukee, WI 53295, USA

ARTICLE INFO

Keywords:
Dorsal horn
Antinociception
Sympathetic nervous system
Cannabinoid
Rat

ABSTRACT

There is growing literature supporting cannabinoids as a potential therapeutic for pain conditions. The development of chronic pain has been associated with reduced concentrations of the endogenous cannabinoid anandamide (AEA) in the midbrain dorsal periaqueductal gray (dPAG), and microinjections of synthetic cannabinoids into the dPAG are antinociceptive. Therefore, the goal of this study was to examine the role of the dPAG in cannabinoid-mediated sensory inhibition. Given that cannabinoids in the dPAG also elicit sympathoexcitation, a secondary goal was to assess coordination between sympathetic and antinociceptive responses. AEA was microinjected into the dPAG while recording single unit activity of wide dynamic range (WDR) dorsal horn neurons (DHNs) evoked by high intensity mechanical stimulation of the hindpaw, concurrently with renal sympathetic nerve activity (RSNA), in anesthetized male rats. AEA microinjected into the dPAG decreased evoked DHN activity (n = 24 units), for half of which AEA also elicited sympathoexcitation. AEA actions were mediated by cannabinoid 1 receptors as confirmed by local pretreatment with the cannabinoid receptor antagonist AM281. dPAG microinjection of the synaptic excitant DL-homocysteic acid (DLH) also decreased evoked DHN activity (n = 27 units), but in all cases this was accompanied by sympathoexcitation. Thus, sensory inhibition elicited from the dPAG is not exclusively linked with sympathoexcitation, suggesting discrete neuronal circuits. The rostrocaudal location of sites may affect evoked responses as AEA produced sensory inhibition without sympathetic effects at 86 % of caudal compared to 25 % of rostral sites, supporting anatomically distinct neurocircuits. These data indicate that spatially selective manipulation of cannabinoid signaling could provide analgesia without potentially harmful autonomic activation.

Introduction

The midbrain periaqueductal gray (PAG) plays a distinct role in pain regulation through descending modulation that enhances or inhibits ascending nociceptive traffic from dorsal horn neurons (DHNs) activated by sensory input from noxious peripheral stimulation (Millan, 2002). The PAG consists of diverse, heterogeneous cell types (Mantyh, 1982b; Beitz, 1985) that are organized into functionally distinct columns around the cerebral aqueduct (Bandler and Shipley, 1994; Carrive, 1993). The dorsal region of the PAG (dPAG) includes dorsomedial, dorsolateral and lateral columns that are associated with active strategies to avoid stressors, including opioid-independent antinociception and sympathoexcitation. In contrast, the ventrolateral PAG is associated with recovery efforts and passive coping related to inescapable pain from deep somatic and visceral sources, opioid-dependent antinociception, pruritis, and sympathoinhibition (Keay et al., 1997; Keay and Bandler, 2001; Samineni et al., 2017; Samineni et al., 2019).

Endogenous cannabinoids (endocannabinoids) are considered viable candidates producing non-opioid analgesia by actions in the dPAG (Starowicz and Finn, 2017). Analgesic efficacy of endocannabinoids is

Abbreviations: AEA, *N*-arachidonylethanolamine, anandamide; CB1R, cannabinoid type one receptor; CV, cardiovascular; DHN, dorsal horn neuron; DLH, DL-homocysteic acid; dPAG, dorsal periaqueductal gray; FAAH, fatty acid amide hydrolase; GPCR, G protein-coupled receptor; IML, intermediolateral cell column; MAP, mean arterial pressure; NTS, nucleus tractus solitarius; PAG, periaqueductal gray; PPAR, peroxisome proliferator activated receptor; RSNA, renal sympathetic nerve activity; RVLM, rostral ventrolateral medulla; RVMM, rostral ventromedial medulla; SIA, stress-induced analgesia; SNS, sympathetic nervous system; TRPV1, transient receptor potential vanilloid type 1; vPAG, ventral periaqueductal gray; WDR, wide dynamic range.

* Corresponding author at: Department of Anesthesiology, Research Service 151, Zablocki VA Medical Center, Milwaukee, WI 53295, USA.
E-mail address: cdean@mcw.edu (C. Dean).

https://doi.org/10.1016/j.ynpai.2022.100104
Received 3 August 2022; Received in revised form 9 September 2022; Accepted 15 September 2022
Available online 16 September 2022

indicated by suppression of hyperalgesia in a rat model of neuropathic pain (Fox et al., 2001). Elevated levels of endocannabinoids in the dPAG following peripheral nerve injury or local stimulation also implicate this region as a critical site of analgesic action (Walker et al., 1999; Petrosino et al., 2007). The synaptic concentrations of the endocannabinoid ligand *N*-arachidonylethanolamine (anandamide or AEA) is regulated by the catabolic enzyme, fatty acid amide hydrolase (FAAH) (Blankman et al., 2007; Cravatt et al., 1996; Egertová et al., 1998; Tsou et al., 1998). Rats that develop sustained hyperalgesia after peripheral nerve injury show increased FAAH transcript and activity, and decreased AEA in the dPAG, suggesting that reduced endocannabinoid signaling in the dPAG contributes to chronic neuropathic pain (Dean et al., 2017). This is consistent with systemic cannabinoids having an antinociceptive effect on wide dynamic range (WDR) dorsal horn neurons (Hohmann et al., 1995) via descending signaling from supraspinal sites (Hohmann et al., 1999), such as the PAG (Martin et al., 1995). However, no studies have been performed to directly assess the ability of endocannabinoids in the dPAG to modulate sensory input at the level of the DHNs.

Stress-induced analgesia (SIA) also increases dPAG endocannabinoid release, while blockade of G-protein coupled cannabinoid 1 receptors (CB1Rs) in the dPAG (Herkenham et al., 1991; Mailleux and Vanderhaeghen, 1992; Tsou et al., 1998) attenuates SIA (Hohmann et al., 2005). Stress initiates integrated responses with the dPAG coordinating sensory and autonomic components by eliciting sympathoexcitation and antinociception that beneficially redirects blood flow to required organs and delays pain responses until an imposed stressor has subsided (Dean and Coote, 1986; Lovick, 1990). Sympathoexcitation, like antinociception, can be evoked by activation of CB1Rs in the dPAG (Dean, 2011a), but it is not known if the cannabinoid-mediated sensory and sympathetic responses are elicited separately or in a coordinated manner.

To address these knowledge gaps, the primary objective of this study was to examine the role of the dPAG in CB1R-mediated sensory inhibition, with a secondary objective of assessing if sensory and sympathetic effects of exogenous AEA in the dPAG are linked. To this end, these experiments tested the effects of dPAG microinjections of AEA on extracellular single unit activity of WDR sensory neurons in the dorsal horn activated by high intensity mechanical stimulation of the hindpaw, simultaneous with renal sympathetic nerve activity (RSNA). The role of CB1Rs in sensory inhibition was examined by local blockade of dPAG CB1Rs prior to AEA microinjection.

Materials and methods

Animals and general surgery

The protocols for this study were approved by the Animal Care and Use Committees at the Medical College of Wisconsin and Zablocki Department of Veterans Affairs Medical Center. All efforts were made to minimize animal suffering and to reduce the number of animals used, but alternatives to in vivo techniques are not suitable for these studies. The experiments were performed in a total of 29 Sprague-Dawley male rats (350–425 gm) obtained from Charles River Labs (Wilmington, MA), anesthetized with sodium pentobarbital (50 mg/kg, i.p.), with a catheter inserted into a femoral vein for supplemental administration of anesthetic doses (2 mg/kg, i.v.). Arterial blood pressure was monitored continuously using a PA-C10 or HD-S10 transmitter (Data Sciences International (DSI), St. Paul, MN) inserted into a femoral artery. The trachea was cannulated through a midline anterior cervical incision for mechanical ventilation (Harvard 683 respirator; Holliston, MA). A surgical plane of anesthesia, characterized by a stable, normal range of blood pressure and RSNA, as well as immobility in response to noxious stimuli was established prior to administration of pancuronium bromide (0.1 mg/kg i.v., with supplemental doses of 0.01 mg/kg administered when spontaneous breathing was observed). Blood pressure and RSNA were monitored continuously, and supplemental doses of anesthetic were administered if abrupt changes in these parameters were observed. A heating pad was used to maintain body temperature at 37 °C.

In vivo electrophysiology

For extracellular DHN recordings, laminectomies were performed at the T13 to L3 vertebrae to expose the L4-L5 levels of the spinal cord. To minimize motion artifact, a stabilizing stereotaxic clamp was attached to the spinal process rostral to the exposure and bilateral pneumothoraxes were performed, after which the animal was mechanically ventilated. The dura was opened and the cord was covered in warm mineral oil. A single barreled glass micropipette containing a carbon filament (7 μm diameter) was advanced into the spinal cord using a microdrive (Burleigh Instruments 6000 Controller, Fishers, NY), targeting lamina IV-VI of the L4-5 level at a depth of 0.6 to 1.2 mm. DHN activity was evoked by repeated mechanical stimulation of the ipsilateral hindpaw. DHNs that responded to low-threshold/non-noxious and high-intensity mechanical stimulation in a graded manner were considered WDR (class 2) neurons and selected for study (Menetrey et al., 1977). Specifically, WDR neurons were identified by their sensitivity to a range of intensities of mechanical stimuli, including light touch with a brush and graded stimuli with von Frey filaments calibrated to 0.04 gm, 6 gm and 60 gm of bending force (Robinson et al., 2014). Filaments were applied to the mid-plantar surface of the hindpaw until a bend was observed. Ten stimulus applications at 1 *sec* intervals were performed for each of the consecutive, graded stimulus intensities (Fig. 1A). The activity of other classes of sensory neurons was not studied.

For sympathetic nerve recordings, a renal nerve was exposed retroperitoneally and positioned on flexible silver wire electrodes. The electrodes were fixed in position with silica gel to provide stability of the recording.

All electrophysiological signals were recorded using high impedance differential amplifiers (gain = 1000; 0.1–10 kHz passband), followed by filter/amplifiers (gain up to 400; high and low pass filtering 10 Hz–3 kHz). The amplifier output was displayed online and also directed to precision full-wave rectifiers and averaged using Bessel linear averaging filters (averaging interval = 100 mS) to obtain an online moving time average. The DHN activity, RSNA, and their moving time averages were continuously sampled at 20 kHz along with arterial blood pressure while displayed and recorded (CED 1401 Power3 and Spike2 data acquisition system, Cambridge Electronic Design Limited, Cambridge, UK).

Microinjection of test agents

With head of the animal fixed in a stereotaxic frame, a dorsal craniotomy was performed and the dura opened to allow the insertion of a multi-barreled glass micropipette (20 μm total tip diameter), attached to a pressure ejection system. Barrels were filled with the synaptic excitant DL-homocysteic acid (DLH; 4 mM; Sigma Chemicals, St. Louis MO) diluted in artificial cerebrospinal fluid (aCSF: in mM; 124 NaCl, 2 KCl, 2 MgCl, 1.3 KH_2PO_4, 0.9 $CaCL_2$, 26 $NaHCO_3$, and 11 glucose); the endocannabinoid and CB1R agonist anandamide diluted in aCSF with 0.01 % Tocrisolve100 (AEA; 50–100 μM; Tocris Cookson, Inc., St. Louis MO); AM281 diluted in aCSF with 3 % Tocrisolve100 (1 μM; Tocris Cookson, Inc., St. Louis MO); aCSF vehicle; Tocrisolve100 vehicle; or pontamine sky blue dye (1 %; VWR International, Radnor PA). DLH is a glutamic acid analog and an NMDA receptor agonist that reliably evokes reproducible responses by activation of neurons in the PAG (Dean, 2011a,b; Bago and Dean, 2001). The micropipette was slowly advanced into the midbrain, targeting the dPAG at coordinates (in mm) ranging from −5.5 to −8.0 from Bregma, 0.2 to 0.8 from midline and 4.0 to 6.0 deep. Initial dPAG microinjection sites were further identified based on physiological responses to DLH using the criteria of RSNA or MAP increase from baseline by a magnitude of at least 20 % or 5 mmHg, respectively. These prespecified thresholds were used to define CV responders and non-responders. The volume of injectate ranged from 7 to

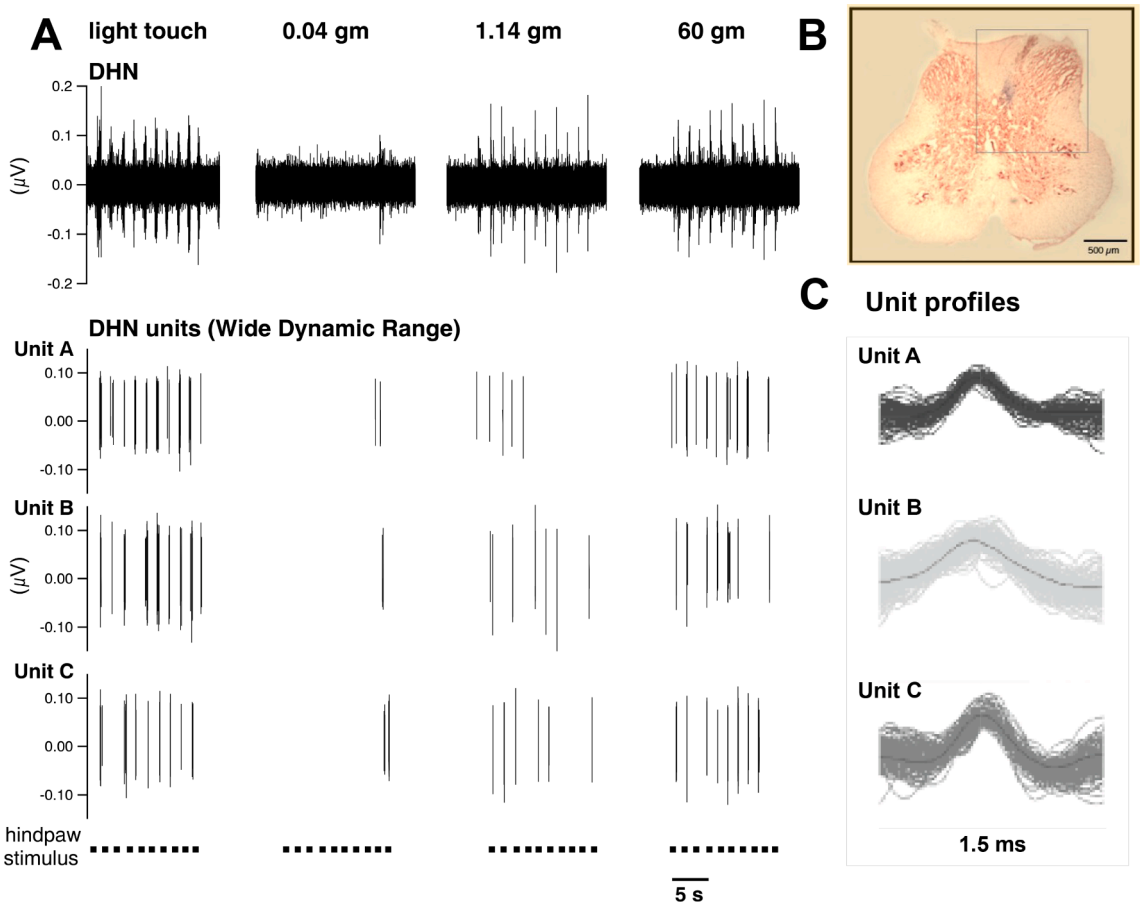

Fig. 1. Identification and sorting of wide dynamic range (WDR) dorsal horn neurons (DHNs). Normally silent WDR neurons are responsive to light touch and graded intensity Von Frey filaments (0.04, 6 and 60 gm) applied to the hind paw receptive field. (A) Extracellularly recorded DHN activity evoked by ten consecutive stimuli to the hindpaw is shown in the upper panel. The lower panels show activity of three separate, WDR neurons (DHN units A-C), with unique responses to graded mechanical stimuli. (B) A WDR DHN recording site marked by dye and indicated by a white arrow is illustrated in Lamina IV of the dorsal horn at L5. (C) Overdrawn spike templates for sorting of DHN units A-C are shown.

50 nanoliters (nl) and was measured by observing the level of the fluid meniscus through a graduated monocular microscope eyepiece (7 nl/div). DHN activity and RSNA were unchanged following vehicle microinjections. Blue dye was microinjected at the most ventral location of a microinjection track for histological recovery. In a subset of animals, a glass micropipette electrode with one recording and one microinjection barrel was used to record DHN activity and microinject dye at dorsal horn sites.

Experimental protocol

After identification of WDR units, DHN activity was evoked at 1 *sec* intervals by mechanical stimulation applied to the receptive field with the 60 gm von Frey filament while RSNA, and blood pressure was monitored continuously. After an initial 20 *sec* von Frey stimulation period for baseline, either AEA or DLH was microinjected at a site in the dPAG, with sensory stimulation continued until monitored parameters returned to baseline levels or for at least 3 min. After recovery of baseline parameters, another microinjection was made at the same site, or the micropipette was advanced 500 μm and the protocol repeated. As a control for adaptation of neuronal units, von Frey mechanical stimulation (60 gm) was applied to the receptive field without drug microinjection (Fig. 2A). Evoked DHN spike rate did not change from baseline at any time point (Fig. 2B). After drug-evoked responses, all parameters returned to baseline prior to examining additional sites.

Histological identification protocol

Brains were removed postmortem and frozen. In the subset of rats microinjected with blue dye at spinal recording sites, the integrity of the cord was maintained by fixation at the end of the study. After perfusion with saline followed by 4 % paraformaldehyde fixative, the brain and spinal cord were removed, post-fixed and frozen. Sequential 25 μm frozen, transverse brain and cord sections were cut, stained with neutral red and examined microscopically to identify dorsal horn recording sites and brain microinjections marked with blue dye. Spinal cord histology confirmed physiological data that DHN recording sites were located in laminae IV-VI of the L4-5 level (Fig. 1B). The depth of multiple PAG microinjections sites in a single track were calculated from the marked ventral site. Rostro-caudal midbrain coordinates are reported as distance from bregma, and diagrammatic representations of the location of midbrain microinjection sites were compiled.

Data analysis

In vivo electrophysiological data were analyzed offline using CED Spike2 version 8 software and imported to SigmaPlot 11 or GraphPad Prism 5 for statistics. Data were extracted from Spike2 to SigmaPlot 11 at a rate of 100 Hz for DHN unit firing rate, average whole RSNA, and mean arterial pressure (MAP). Spike2 software was used to extract single DHN units from evoked bursts of ensemble DHN activity based on template matching and principal component analysis, allowing identification of one to four WDR DHN units for each recording site (Fig. 1C).

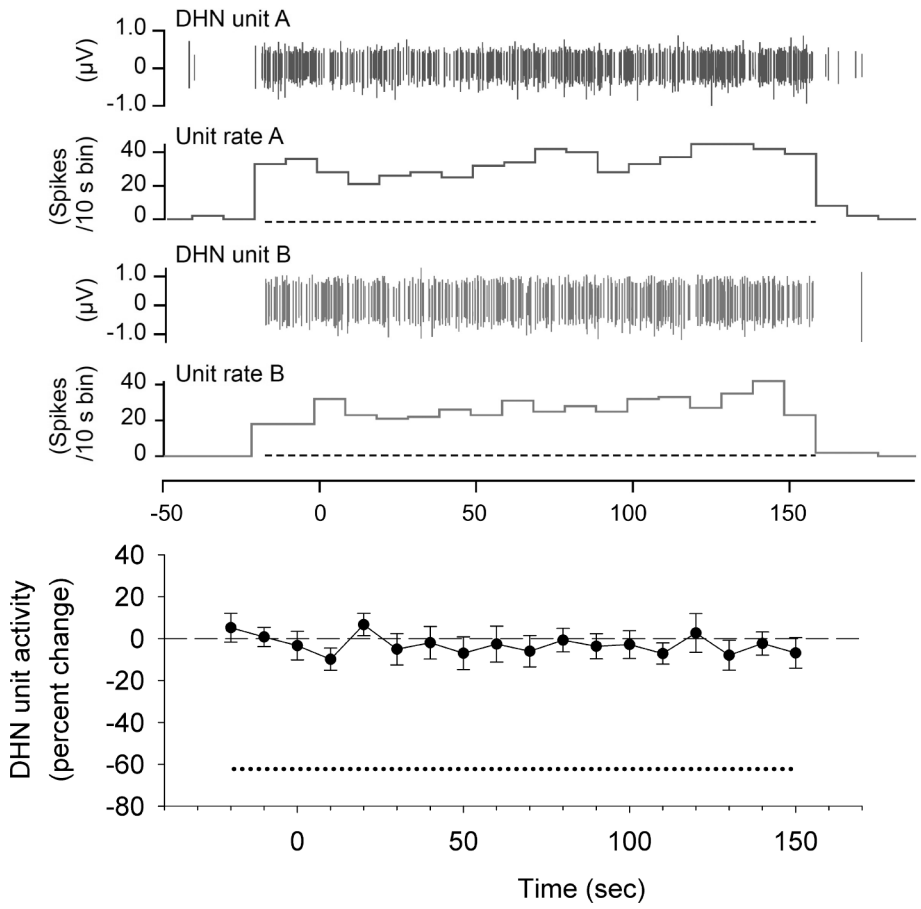

Fig. 2. Stable firing rate of WDR DHNs. Repeated von Frey (60 gm) stimulation (indicated by dashed lines) of the receptive field on the hindpaw evoked stable rate of firing of WDR DHN units. A) Units A and B do not adapt to sustained high-intensity mechanical stimulation. B) Group data show that DHN spike rate during mechanical stimulation does not change with time ($F_{16,18} = 0.5$; $p > 0.05$) or at any time point ($p > 0.05$; $N = 17$).

Baseline values for evoked firing frequency of DHNs, which were altered by dPAG microinjections, ranged from 0.5 to 14.5 Hz with a mean of 3.0 and a median of 2.3 Hz. To eliminate noise from RSNA, zero activity was obtained at the end of the experiment by crushing the nerve proximal to the recording electrodes, averaging the remaining noise level, and subtracting it from the averaged activity.

Statistical analysis

A moveable cursor was set at the onset of an experimental protocol to act as a zero-time marker for the analysis. Data were collected and averaged in sequential 10 *sec* periods from 50 *sec* prior to microinjection (30 *sec* without hindpaw stimulation and 20 *sec* baseline with von Frey stimulation). DHN unit firing rate and RSNA in 10 *sec* bins were subsequently expressed as percent changes from mean baseline bins preceding each dPAG microinjection. A decrease in DHN unit activity was defined by a decrease from baseline with a magnitude of at least 20 %. For each 10 *sec* period after microinjection, DHN unit activity, RSNA and MAP were compared using repeated measures one-way ANOVA. Significantly different means were identified using Holm-Sidak planned *post-hoc* comparisons with significance set at $P < 0.05$. Spearman correlation was used to determine the degree of association between trough DHN unit activity and maximum RSNA and to calculate the coefficient of determination (r^2). Fisher's exact test assessed the proportion of observations in which sensory changes were found in isolation or in combination with sympathetic changes to determine if the rostro-caudal distribution of those two patterns were equally likely. Data are reported as mean ± SD unless noted otherwise.

A lack of centrally-evoked change in DHN unit activity could be meaningful but could also reflect that the dorsal horn recording site is not in the projection field of that dPAG microinjection site. In this study, 97 WDR DHN units showed no response after microinjection of either AEA or DLH at 58 dPAG sites. These data are not further considered here given that there is no clear somatotopic organization (homunculus) within the PAG.

Results

Sensory inhibition follows dPAG AEA injection

AEA microinjection at 16 dPAG sites decreased evoked unit firing rate in 24 dorsal horn WDR neurons (Fig. 3A; Unit A), while activity of other units sorted from the same recording were unchanged (Fig. 3A; Unit B) and none increased discharge rate. The nadir in DHN firing rate for those responding was −38.8 ± 29.7 % at 130 *sec* after microinjection (Fig. 3A; bottom panel) demonstrating that dPAG AEA inhibits mechanically evoked firing of WDR DHNs.

Sensory inhibition follows dPAG DLH injection

DLH microinjection at 21 dPAG sites decreased unit firing rate in 27 dorsal horn WDR neurons. While evoked activity of some DHNs were inhibited (Fig. 3B; Unit A), other units sorted from the same dorsal horn recording were unchanged (Fig. 3B; Unit B) and none increased discharge rate. The nadir in DHN firing rate for those responding was −39.2 ± 28.5 % at 70 *sec* after microinjection (Fig. 3B; bottom panel).

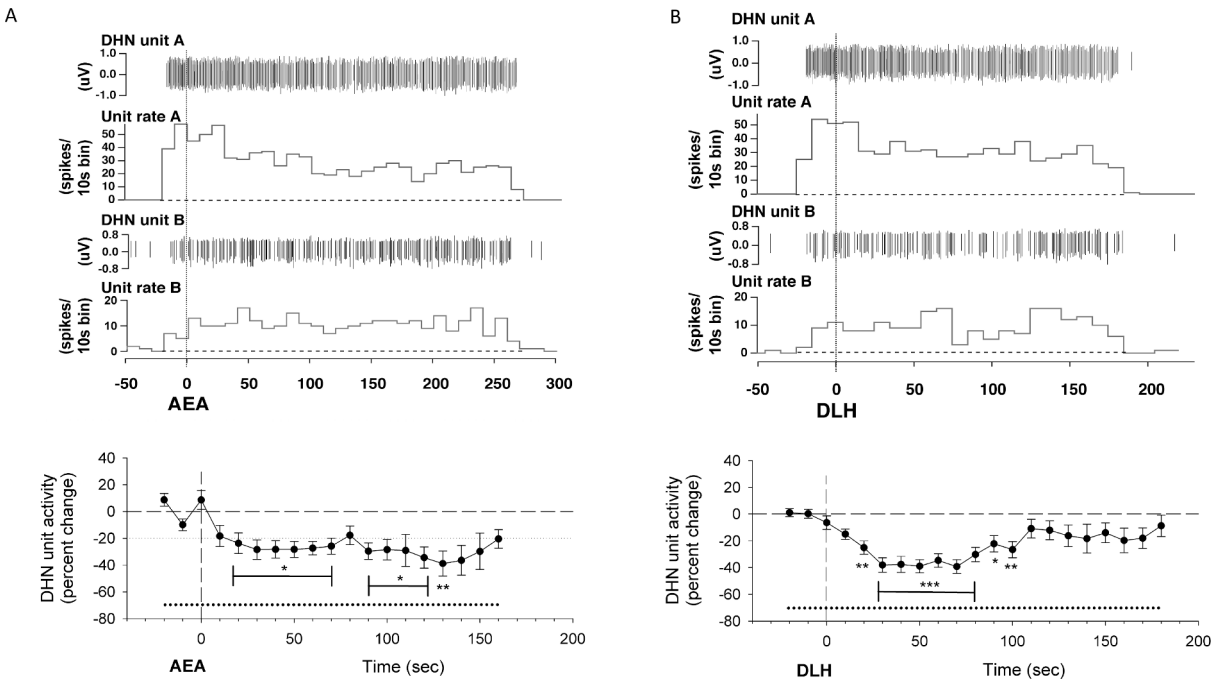

Fig. 3. Sensory responses to microinjection of anandamide (AEA; 2–5 pmol) and DL-homocysteic acid (DLH; 56–112 pmol) in the dorsal periaqueductal gray (dPAG). A) In one neuron (Unit A; top panel) AEA microinjection evokes a decrease in DHN unit discharges evoked in response to hindpaw high-intensity stimulation. In another DHN (Unit B; middle panel) discharge rate does not change. After AEA microinjection, DHN spikes significantly decrease with time (bottom panel; $F_{21,23} = 4.0$; $p < 0.001$; $n = 24$). B) A separate DLH microinjection at the same dPAG site evokes a similar pattern of responses in these units (top and middle panels). After DLH microinjection, DHN spikes significantly decrease with time ($F_{21,26} = 7.9$; $p < 0.001$; $n = 27$) according to repeated measures One-way ANOVA (bottom panel). All DHN WDR activity was evoked in response to von Frey stimulation of the receptive field of the hindpaw indicated by dashed horizontal lines. Post-hoc planned comparisons by Holm-Sidak method shows DHN Spikes significantly decrease from baseline (***$p < 0.001$; **$p < 0.01$; and *$p < 0.05$ compared to time zero) at each of the designated time points.

DHN responses to either AEA or DLH are different

The DHN responses to dPAG microinjections of AEA or DLH were examined when each drug was tested individually at the same dPAG location. Out of 26 dPAG:DHN unit pairs, AEA resulted in sensory inhibition of a total of 15 units of which 9 were distinct responses not elicited with DLH. Likewise, DLH caused sensory inhibition in 17 DHNs with 11 distinct sensory inhibition responses not elicited by AEA. In 6 instances (23 %), AEA and DLH had the same effect on the dPAG:DHN unit pairs (Fig. 4).

DHN activity following AEA is dependent on CB1R signaling

In a subset of experiments, 4 dorsal horn WDR neurons that decreased firing rate after AEA microinjection at 4 dPAG sites were further tested to determine the contribution of CB1R signaling. The nadir in DHN firing rate after dPAG administration of AEA was −69.7 ± 19.0 % at 150 *sec* after microinjection (Fig. 5A). After baseline parameters were recovered and 5 min following AM281 microinjection at the same dPAG site, repeat microinjection of AEA yielded no significant change in DHN unit activity (Fig. 5B). After 60 min of recovery, the effect of AEA to decrease DHN firing rate was partially restored, such that the nadir in DHN firing rate after AEA was −63.1 ± 12.4 % at 70 *sec* after microinjection (Fig. 5C).

Sympathoexcitation follows dPAG AEA injection

AEA microinjection at 17 dPAG sites increased renal sympathetic outflow (Fig. 6A; top panels). The maximum increase in RSNA was 17.8 ± 55.9 % at 30 *sec* after microinjection. MAP also increased to 110 ± 15.4 mmHg from a baseline value of 105 ± 13.0 mmHg (Fig. 6A; bottom panels).

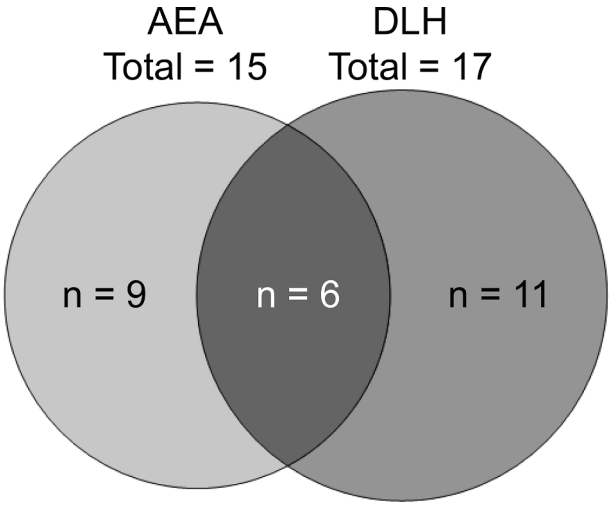

Fig. 4. Sensory inhibition elicited by dPAG microinjections of AEA and DLH. Response patterns were unique when each drug was individually tested at the same site. The Venn diagram illustrates that 6 of 26 (23%) dPAG:DHN spike unit pairs resulted in the same response to AEA and DLH, whereas 20 of 26 (77%) had distinct responses.

Sympathoexcitation follows dPAG DLH injection

DLH microinjection at 22 dPAG sites increased RSNA (Fig. 6B; top panels) with a maximum increase of 75.5 ± 68.5 % at 20 *sec* after microinjection (Fig. 6B; bottom panels). The peak MAP was 118 ± 13.5 mmHg increased from a baseline value of 104 ± 11.0 mmHg.

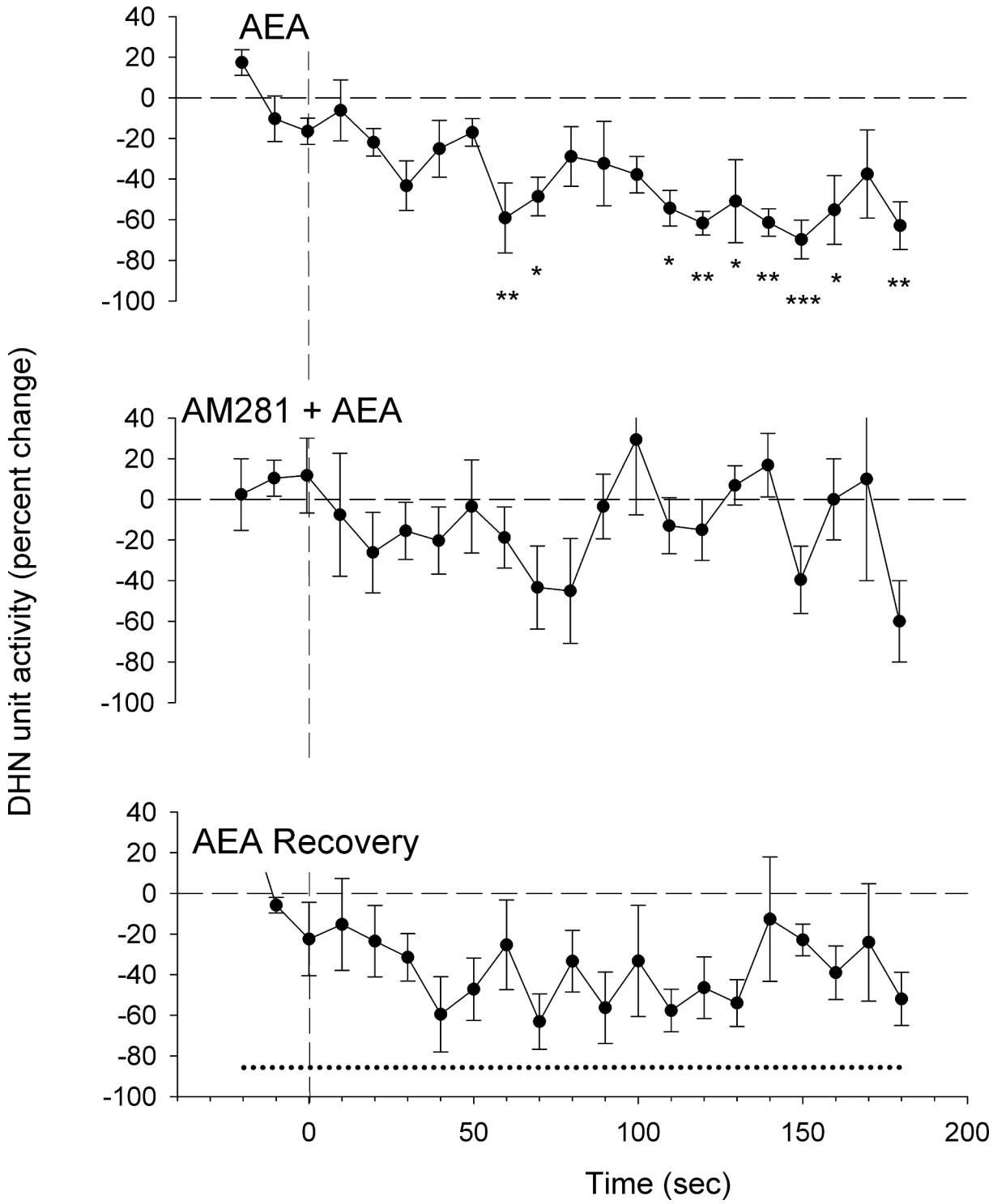

Fig. 5. Sensory responses to microinjection of AEA (2–5 pmol) in the dPAG were blocked by the CB1R antagonist, AM281 (1 μM). A) AEA microinjection significantly decreased DHN spikes over time ($F_{3,21} = 4.5$; $p < 0.001$). B) AEA microinjection at the same dPAG site, 5 min after microinjection of AM281 did not change DHN spikes over time ($F_{3,21} = 1.4$; $p > 0.05$). C) Following a 60 min recovery from AM281 microinjection, AEA microinjection at the same dPAG site significantly decreased DHN spikes over time ($F_{3,21} = 3.1$; $p < 0.001$; $n = 4$). All DHN WDR activity was evoked in response to von Frey stimulation of the receptive field of the hindpaw indicated by dashed horizontal lines. Post-hoc planned comparisons by Holm-Sidak method shows DHN Spikes significantly decrease from baseline (***$p < 0.001$; **$p < 0.01$; and *$p < 0.05$ compared to time zero) at each of the designated time points.

Sympathetic nerve activity and arterial pressure responses to DLH are not always replicated by AEA

The observed sympathetic responses to dPAG microinjections of AEA and DLH were consistent with our previously published work that demonstrated typical increases in RSNA and MAP in the magnitude of 20–150 %, and 5–20 % respectively (Dean, 2011a,b). Similar to prior studies (Dean, 2011a,b), when AEA evoked a sympathetic response at a given site, a similar response was evoked by DLH without exception (n = 8). In contrast, DLH-induced sympathoexcitation was not always

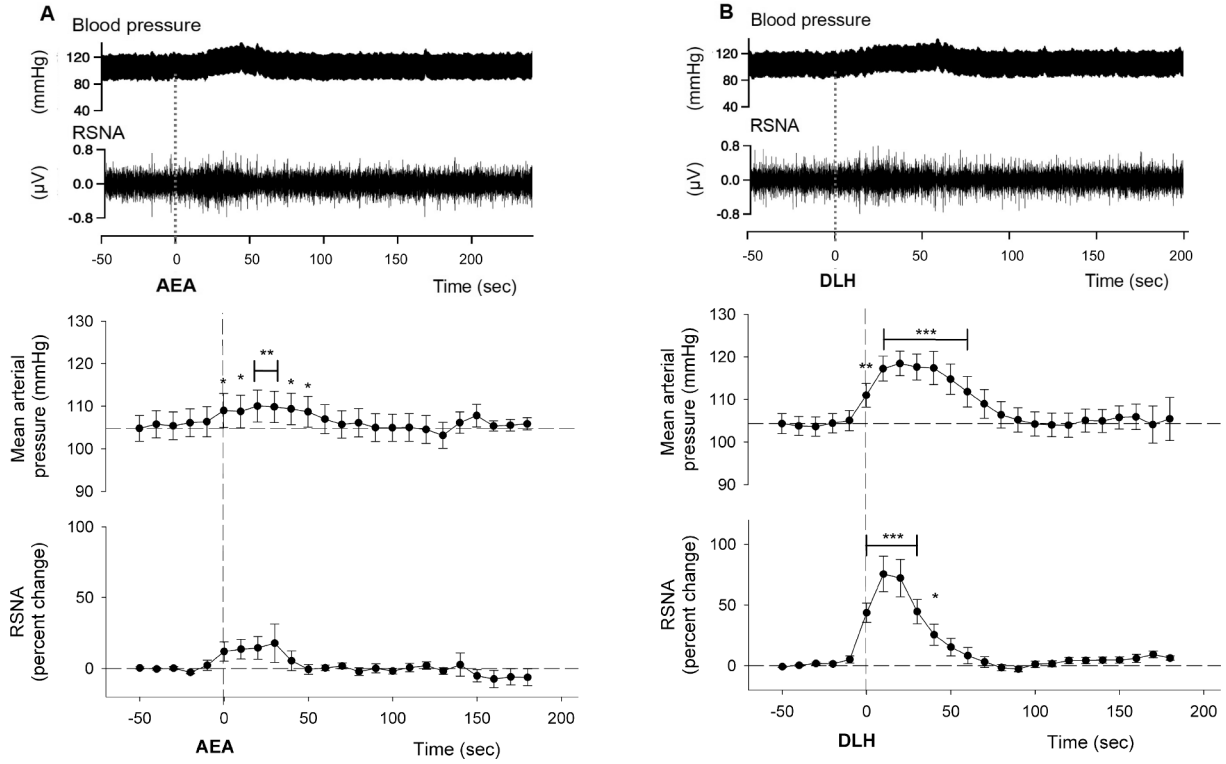

Fig. 6. Cardiovascular (CV) responses to microinjection of AEA (2–5 pmol) and DLH (56–112 pmol) in the dPAG. A) At one microinjection site (top panel), AEA evokes an increase in blood pressure and renal sympathetic nerve activity (RSNA). Following AEA, arterial pressure ($F_{16,23} = 4.2$; $p < 0.001$) and RSNA ($F_{16,23} = 1.7$; $p < 0.05$) increases with time according to repeated measures One-way ANOVA (bottom panel) and at each of the designated time points (***$p < 0.001$; **$p < 0.01$; *$p < 0.05$; $n = 17$). B) A separate microinjection of DLH, at the same dPAG site, evokes increases in blood pressure and RSNA. After DLH microinjection, arterial pressure ($F_{21,23} = 19.9$; $p < 0.001$) and RSNA ($F_{21,23} = 16.3$; $p < 0.001$) increases with time according to repeated measures One-way ANOVA (bottom panel) and at each of the designated time points (***$p < 0.001$; **$p < 0.01$; *$p < 0.05$; $n = 22$).

imitated by AEA ($n = 20$). This finding demonstrates different responses of the two drugs (Fig. 7A). Specifically, there was a group of dPAG sites that responded to AEA with changes very similar to the sympathoexcitation elicited by DLH and another group of dPAG sites at which AEA evoked minimal RSNA or MAP changes.

Sensory inhibition and sympathoexcitation after AEA are not linked

AEA microinjected at 8 dPAG sites evoked a decrease in unit activity of 24 WDR DHNs, of which 12 were associated with an increase in RSNA (Pattern 1; Fig. 7B). For the response pattern with concurrent sensory inhibition and sympathoexcitation, the nadir in sensory inhibition was

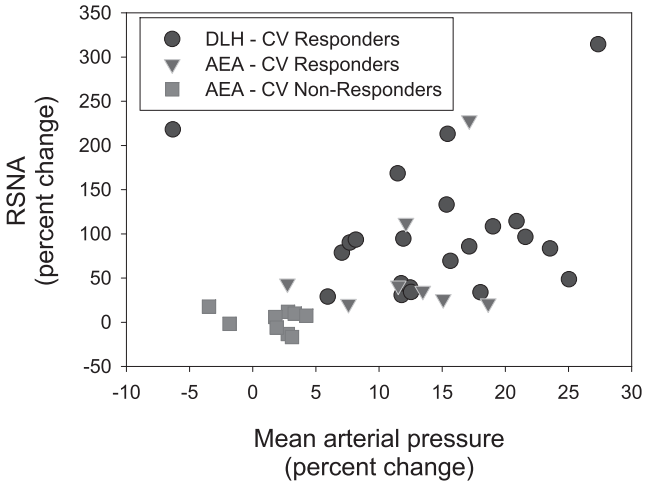

Fig. 7. Differential CV responses to dPAG microinjection of AEA (2–5 pmol) and DLH (56–112 pmol). A) Responses of mean arterial pressure (MAP) and RSNA are heterogenous for both AEA and DLH where sensory changes were evoked. Analysis of the two subgroups of AEA responses yielded B) a group of CV responders that have RSNA ($F_{7,23} = 1.6$; $p < 0.05$) and MAP ($F_{7,23} = 4.1$; $p < 0.001$) increases with time and MAP significantly increases at designated time points (**$p < 0.01$ and *$p < 0.05$) after injection ($n = 8$). In contrast, a group of CV non-responders C) have no change in either RSNA ($F_{8,18} = 0.7$; $p > 0.05$) or MAP ($F_{8,18} = 1.5$; $p > 0.05$) after microinjection ($n = 9$). AEA microinjection resulted in a main effect of a decrease in WDR DHNs activity in both the CV responders ($F_{11,21} = 2.5$; $p < 0.001$) and non-responders ($F_{11,16} = 2.3$; $p < 0.01$) and at designated time points after injection.

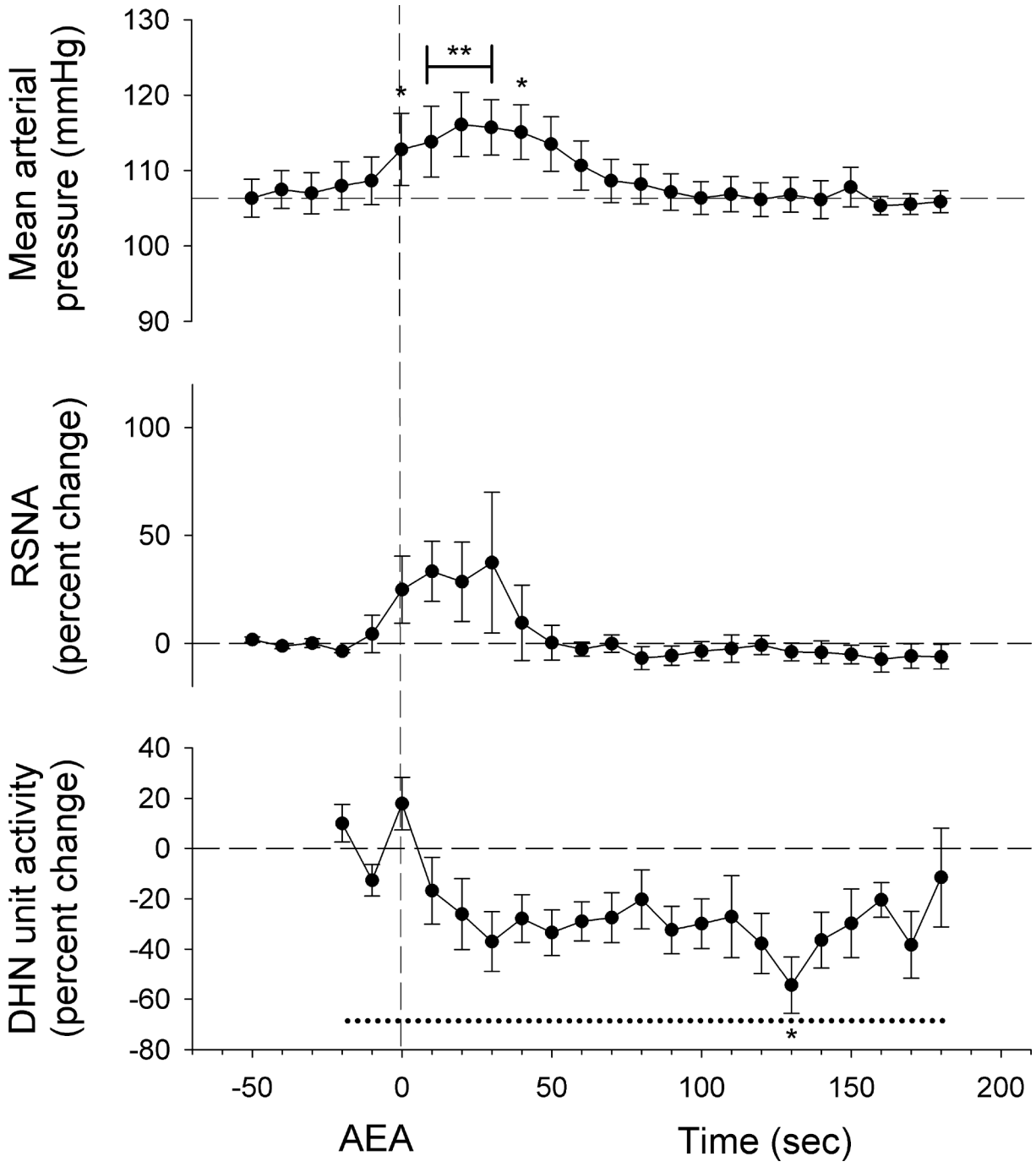

Fig. 7. (*continued*).

−54.3 ± 27.5 % at 130 *sec* after microinjection and the peak RSNA was 36.5 ± 79.8 % at 30 *sec* after microinjection. To further examine whether the DHN and RSNA responses are interrelated, the nadir in the absolute value of the percent change of DHN activity was compared to the maximal percent change in RSNA after dPAG pharmacological manipulation with AEA. There was no significant correlation between the trough in DHN firing rate and the maximum change in RSNA (r^2 = 0.11, Fig. 8), suggesting that these variables are independent.

RSNA was not always affected by dPAG microinjection of AEA that reduced DHN responses to von Frey stimulation (Pattern 2; Fig. 7C). Specifically, at 9 dPAG sites AEA evoked a decrease in firing rate of 12 dorsal horn WDR neurons (nadir of −33.5 ± 34.3 % at 110 *sec* after microinjection) without a change in RSNA or MAP.

Sensory inhibition and sympathoexcitation after DLH are not linked

At all dPAG sites at which microinjections of DLH caused a decrease in DHN unit firing rate, RSNA and MAP were increased. Although all dPAG areas that demonstrated sensory inhibition in response to DLH also caused sympathoexcitation, these variables are independent (r^2 = 0.04, Fig. 8).

Histology correlation with physiological responses

Histologically-verified dPAG sites (Fig. 9A/B) from which AEA or DLH evoked decreases in DHN firing rate were dispersed throughout the dorsomedial, dorsolateral and lateral regions extending from −5.0 to

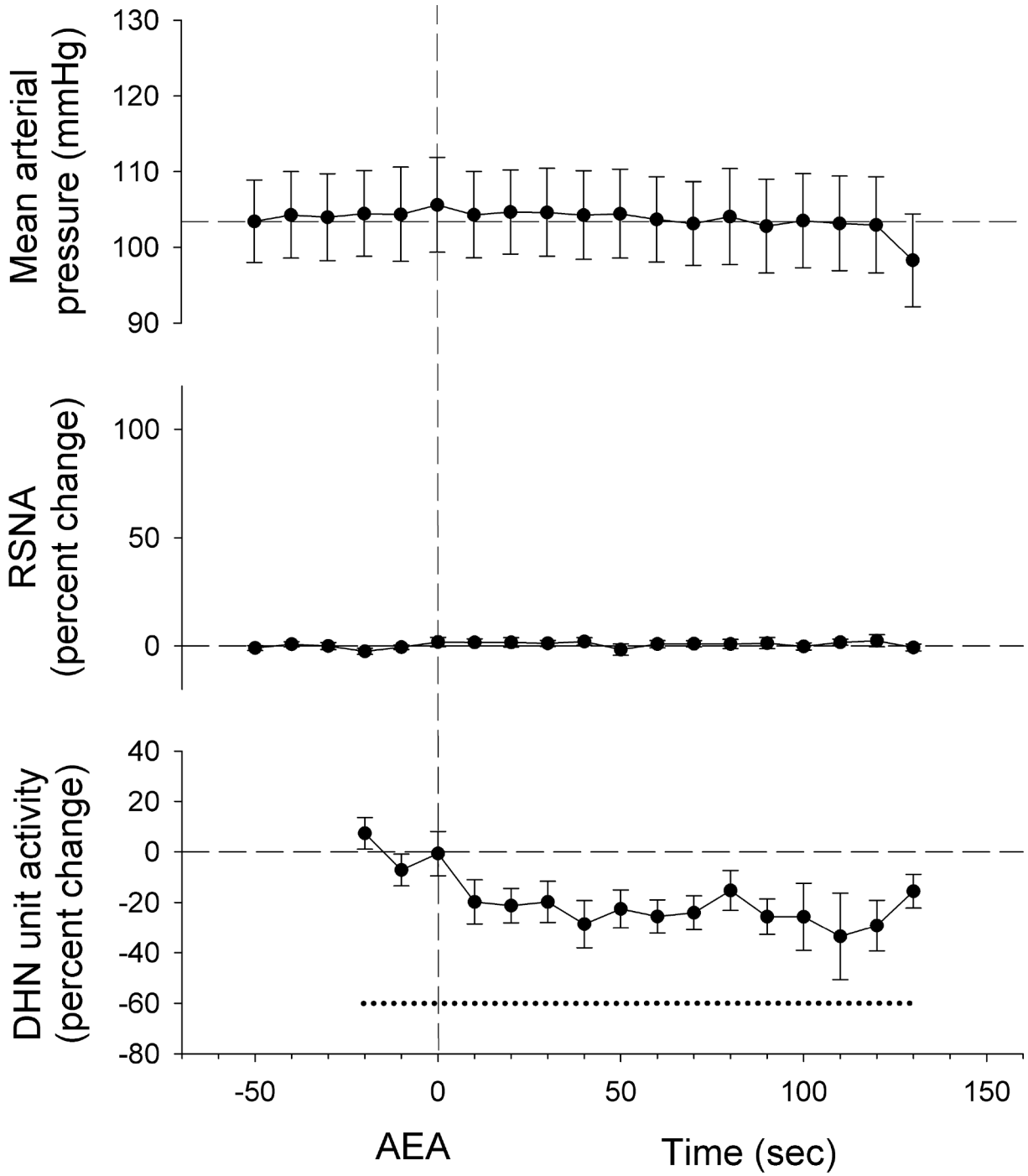

Fig. 7. (*continued*).

−8.0 mm caudally from bregma (Fig. 9C). The response to AEA resulted in sensory inhibition without sympathetic effects at 6 out of 7 (86 %) dPAG microinjection sites that were caudal to −6.5 mm. At regions rostral to −6.5 mm, AEA evoked coordinated sympathetic and sensory responses at 6 of 8 (75 %) sites. Given that DHN and RSNA changes after dPAG microinjections are independent (Fig. 8), this rostrocaudal distribution of sensory changes compared to coordinated effects was tested for the null hypothesis that response patterns 1 (Fig. 7B) and 2 (Fig. 7C) are equally likely to occur rostral and caudal to −6.5 mm from Bregma. Fischer's exact test ($p = 0.04$) suggests there is a 96 % probability that this anatomical pattern would not be observed by chance.

Discussion

This study directly demonstrates that exogenous administration of the endocannabinoid AEA into the dPAG inhibits sensory input to the dorsal horn via central CB1Rs. The sensory physiology data presented here are congruent with systemic cannabinoids having an antinociceptive effect (Starowicz and Finn, 2017; Fox et al., 2001), which have been shown to decrease WDR DHN firing rate (Hohmann et al., 1995) via descending signaling from supraspinal sites (Hohmann et al., 1999) including the dPAG (Martin et al., 1995). Our novel finding is also consistent with prior studies that demonstrate reduced endocannabinoid signaling in the dPAG in chronic neuropathic pain models (Dean et al., 2017). Together, these observations indicate that CB1R activation may

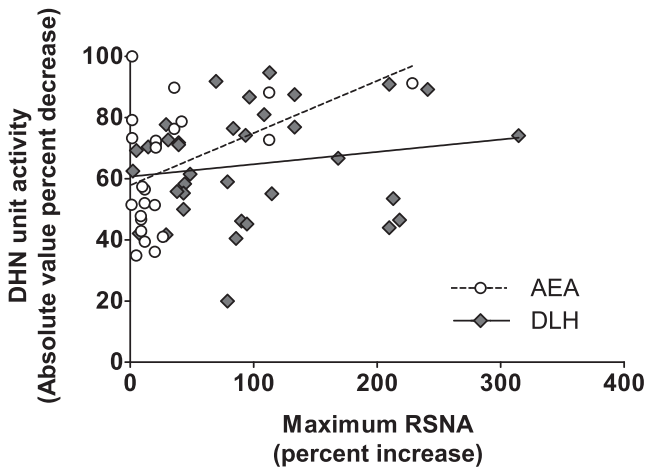

Fig. 8. Lack of association between the peak decrease in evoked DHN firing rate and the maximum increase in RSNA. Spearman correlation indicates that the absolute value of the percent decrease in DHN spike frequency and the percent increase in RSNA do not exhibit a monophasic relationship for either AEA (white circles; $r = 0.33$; $p > 0.05$) or DLH (gray diamonds; $r = 0.20$; $p > 0.05$) microinjections into the dPAG.

be a viable analgesic treatment option.

Sensory inhibition evoked by AEA was blocked by AM281, indicating that it is primarily mediated by CB1Rs in the dPAG. Other studies have demonstrated that CB1R antagonists block 60–80 % of the analgesia evoked by cannabinoid agonists or SIA, which increases AEA in the PAG (Hohmann et al., 2005; Walker et al., 1999). This reproducible degree of reversal could be due to incomplete pharmacological antagonism, but does not rule out a contribution from other receptors that might have a minor role, such as the transient receptor potential vanilloid type 1 (TRPV1), peroxisome proliferator activated receptors (PPARs), and orphan G protein-coupled receptors (GPCRs) (Ross, 2003; O'Sullivan, 2007; Godlewski et al., 2009; Okine et al., 2019). TRPV1 mediates analgesia from the PAG (Palazzo et al., 2002; Maione et al., 2006; Xing and Li, 2007), but the pmol dosage of AEA used in the present studies corresponds to the range for CB1R activation, which is at least 100-fold lower than required for TRPV1 (Ross, 2003; Pertwee, 2005; Lisboa and Guimaraes, 2012).

Data from this study support cannabinergic involvement in the mediation of an acute stress response since AEA can elicit coordinated sensory inhibition and sympathoexcitation from the dPAG. This is consistent with the historical view of the dPAG as an integrative region that assimilates multiple inputs into appropriately graded analgesic and pressor effects (Dampney, 2015). Similar to the sensory inhibition observed here, dPAG- and hypothalamus-evoked sympathoexcitation are also attenuated by AM281, demonstrating a CB1R mechanism (Dean, 2011a). These data suggest that sensory inhibition and sympathoexcitation are mediated by the same receptors, but does not conclusively rule out the involvement of additional, different receptors in the sensory and autonomic networks.

This study sheds light on the dPAG-spinal circuits mediating coordinated neural responses. The magnitude of AEA and DLH effects on RSNA and MAP (Fig. 6A/B bottom panels) are different because dPAG locations where AEA inhibited sensory signaling was comprised of a group of cardiovascular responders and non-responders (Fig. 7A), which would be consistent with distinct neuronal pathways. AEA evoking descending inhibition of sensory inputs from the dPAG in the absence of autonomic activation of either blood pressure or RSNA (Fig. 7C) is supportive of the existence of unique neurocircuits. The above findings suggest that although the analgesic and autonomic pathways could be linked in some physiological states (Fig. 7B), they can also be activated separately. This hypothesis is further supported by the lack of a correlation between antinociceptive and sympathetic responses for either AEA or DLH in this study (Fig. 8), and is compatible with human deep brain stimulation in which electrodes in the dPAG that achieve analgesia are accompanied by blood pressure increases in only a quarter of the patients (Green et al., 2006). The present study supports an anatomical basis for this separation in our studies, given that AEA resulted in sensory inhibition without sympathetic effects at more caudal dPAG sites at a frequency beyond what would be expected by chance (Fig. 9). While sympathoexcitation without sensory inhibition was elicited by AEA microinjection in the dPAG, these data cannot be reliably interpreted due to study design and methodological limitations. This pattern of response could be a true finding with no sensory control from the dPAG microinjection site, but could also be a false-negative if the evoked DHN unit is not in the projection field of the activated dPAG neurons. Therefore, these findings were excluded from analyses. Nevertheless, the anatomical findings presented here are intriguing given a previous report that formalin-induced increases in Fos expression in the caudal lateral PAG was attenuated by dPAG injection of a cannabinoid agonist, which also decreased nociceptive behaviors (Finn et al., 2003). The data described, but not shown in that manuscript, found that $n = 5$ microinjections into the lateral column of the PAG had no effect on formalin-evoked nociceptive behavior, which is challenging to compare to the present study without further histological information. Although prior tracer studies in rats have been relatively equivocal regarding topographical associations between PAG and DHN sites (Cameron et al., 1995; Mantyh, 1983a; Mantyh and Peschanski, 1982), there is growing evidence that cannabinoids exert antinociceptive mechanisms via descending signaling from supraspinal sites (Hohmann et al., 1999), including the PAG (Martin et al., 1995; Finn et al., 2003), and that these neurocircuits are independent of motor (Martin et al., 1996) and autonomic pathways, which would be consistent with the findings presented here. Neither the histological evaluations of CB1Rs in the PAG already published (Herkenham et al., 1991; Mailleux and Vanderhaeghen, 1992; Tsou et al., 1998) nor the data presented here, have the anatomical resolution to determine if the CB1R expression pattern could explain the diverse physiological responses in this dataset, which is not surprising given the heterogenous nature of the PAG. Taken together, these data support the theory that autonomic outflow can be controlled independently from antinociception within dPAG neurocircuitry, but a pragmatic methodology of accomplishing this goal has not yet been determined.

The detailed organization of the dPAG neurocircuitry mediating our observed responses is not known, but our findings provide new insights. While our data support the idea that analgesic and sympathetic pathways consist of two parallel circuits with close anatomic proximity in the dPAG, we cannot rule out alternatives, such as, one pathway with divergent outputs to sensory and autonomic targets. Two parallel circuits would be the simplest that could account for both AEA-induced patterns of response observed here. Microinjections limited to neurons mediating analgesia could elicit sensory inhibition alone, but spread of injectate also encompassing neurons regulating sympathetic activity would result in both sensory and sympathetic effects. This would suggest that although minimal drug volumes (7–50 nl) were microinjected, spread of injectate could be a limiting factor in these experiments given that the PAG is a notoriously heterogeneous mosaic of cell types and signaling processes (Millan, 2002; Keay et al., 1997; Keay and Bandler, 2001; Behbehani, 1995; Heinricher et al., 2009). AEA injectates may have a smaller functional range than DLH since AEA is rapidly inactivated by FAAH, which limits accumulation and spread (Cravatt et al., 1996; Egertová et al., 1998). If future studies can demonstrate that a single neuron controls both sensory inhibition and sympathetic outputs, while opposite to the distinct neuronal pathways proposed here, then those results taken together with these studies would suggest that axons from the same neuron with divergent functions can be activated independently. Selective axon activation could happen by a number of mechanisms, such as actions at subcellular neuronal compartments,

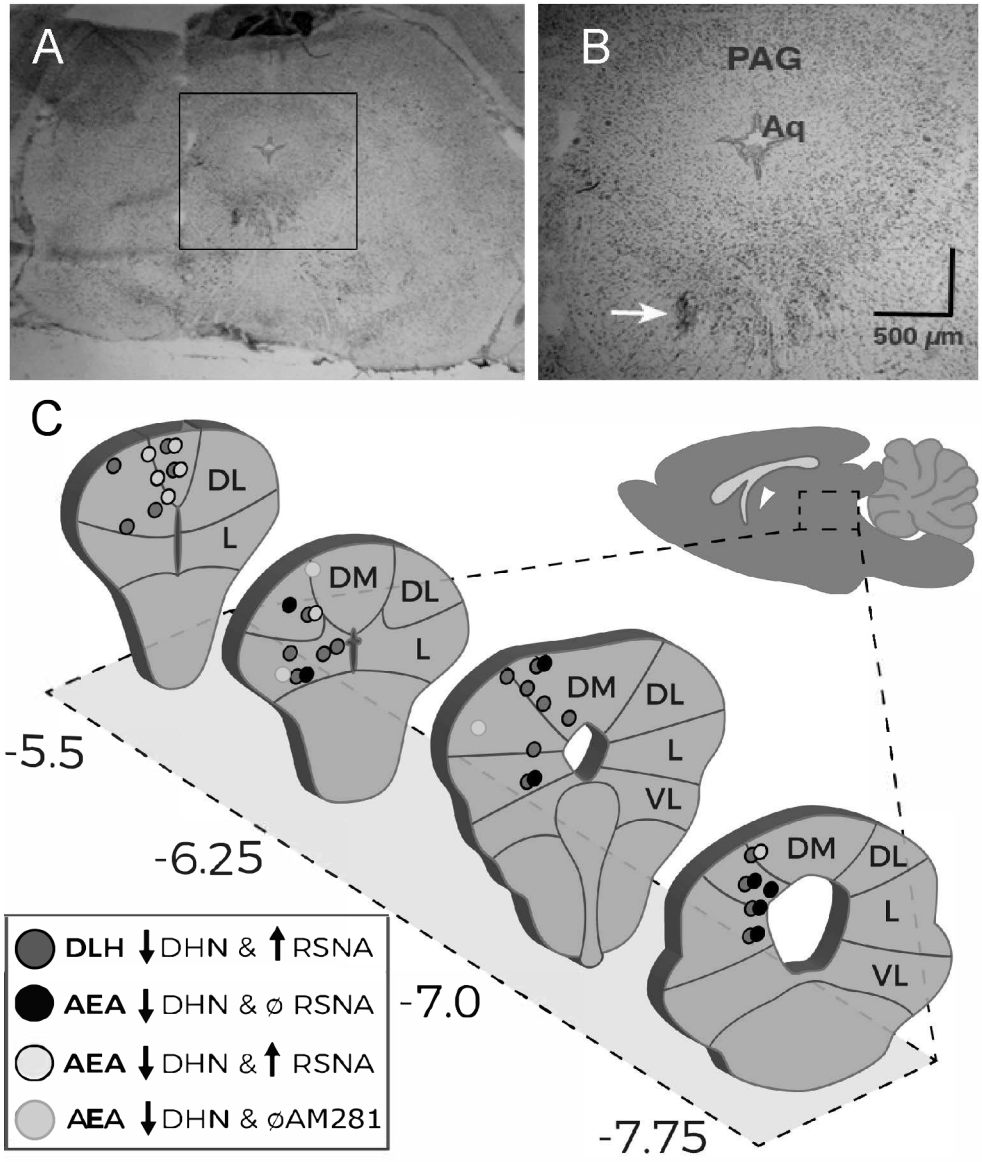

Fig. 9. Histological localization of midbrain microinjection sites. Low power (A) and high power (B) magnification of a section of the midbrain illustrates dye on the ventral border of the PAG (white arrow in B), marking the most ventral site of a PAG track. Microinjections were made at 500 μm depth intervals. A schematic representation of the PAG (C) illustrates microinjection sites from which AEA elicited a decrease in DHN unit discharges without a change in RSNA (black circles) or in association with an increase in RSNA (light gray circles) and from which DLH evoked a decrease in DHN firing rate and increase in RSNA (dark gray circles). Sites where AM281 blocked AEA effects are marked (medium gray circles). Histologically recovered sites ranged from −5.0 to −8.0 mm from bregma and are displayed on the closest section.

modification of intracellular signals (second messengers, kinases or ion channels) that predominantly activate one pathway, or a greater degree of activation being required in order to have measurable changes in sympathetic outflow compared to sensory inhibition. Another alternative that has not been definitively ruled out is that a single neurocircuit mediates the sympathoexcitation and sensory inhibition via different receptors. In this scenario, these different receptors would both have to be responsive to AEA and dependent on AM281, which has been shown here for sensory inhibition and in previously published data for sympathoexcitation (Dean, 2011a). Different receptors could entail unique subtypes or post-translational modifications, as well as, distinct receptor populations, for example, within separate synaptic microenvironments (Shiosaka and Yoshida, 2000). CB1R activation of different anatomical sites or intertwined neurocircuits remains most likely, but further studies are warranted to elucidate an intervention for segregating these pathways, given that doing so could provide a promising opportunity for targeted cannabinergic therapy that would provide analgesia without unwanted autonomic and cardiovascular effects.

Prior studies (Dean, 2011a,b) demonstrate that AEA-induced CB1R activation in the dPAG inhibits tonically active GABAergic neurons to enhance glutamatergic outflow related to sympathoexcitation. Whole cell patch clamp recording in PAG slices also demonstrates AEA-mediated suppression of GABAergic neurotransmission via the CB1R, although function could not be assigned to these neurons (Lau et al., 2014). Therefore, while AEA acts indirectly through disinhibition, DLH directly activates glutamatergic projection neurons to enhance sympathetic outflow (Dean, 2011a,b). This could explain how AEA and DLH evoke similar response patterns at the same dPAG site, but also why DLH is effective at many sites where AEA is not. The current working hypothesis, based on the above literature and the data presented here, is that AEA-induced CB1R-mediated sensory inhibition has a similar mechanism. In the absence of evidence to the contrary, retrograde synaptic signaling of endocannabinoids that acts indirectly to cause disinhibition is the most likely synaptic and cellular mechanism responsible for sensory inhibition. Overall, these results are consistent with, and build on, prior studies of the effects of exogenous AEA in the dPAG on sympathetic outflow (Dean, 2011a,b), but the same mechanisms may not be responsible for descending inhibition of sensory inputs so further studies are warranted.

The time course characteristics of the analgesic and sympathetic responses in this study offer additional support for distinct pathways for their effects consistent with other investigators observations (Hohmann

et al., 1999; Martin et al., 1996). The neural connections for the PAG-to-dorsal horn and the PAG-to-intermediolateral cell column circuits are complex (Millan, 2002; Dampney, 2015). There are numerous connections by which the midbrain can cause descending inhibition of sensory inputs, including via pontine and medullary regions, such as the nucleus tractus solitarius, parabrachial nucleus, and rostoventromedial medulla (Cameron et al., 1995). Interestingly, the PAG does have a population of nerve fibers that directly project to DHNs of the spinal cord, and some spinal cord afferents project directly to the PAG (Millan, 2002; Keay et al., 1997; Mantyh, 1983; Mantyh, 1982a). However, the time course of DLH-induced analgesic responses reported here is consistent with prior studies showing an onset within 30 *sec* and an action that persists for less than 3 min (Waters and Lumb, 1997). Therefore, it is unlikely that a direct PAG-to-DHN connection is solely responsible for our results given that the time course of WDR neuron changes are slower relative to RSNA/MAP changes, which begin within 10 *sec* and resolve within a minute. The pathways mediating the dPAG output to the sympathetic efferents could involve the dorsal medial hypothalamus, nucleus tractus solitarius, caudal or rostral ventrolateral medulla, to the intermediolateral cell column, which innervates end organs (Dampney, 2015; Lovick, 1993; Farkas et al., 1998). Potential explanations for why sensory responses lag behind sympathetic, beyond different neurocircuits, include differences in synaptic types (axodendritic, axosomatic, axoaxonic), speed of action potential propagation (myelinated versus unmyelinated fibers), or temporal characteristics of neurotransmitter systems along the descending pathway (e.g. exocytosis, diffusion, recycling or post-synaptic receptor coupling (Cui et al., 1999; Peng et al., 1996a–c). Alternatively, but not mutually exclusive to the above, the PAG-to-dorsal horn network may have more synaptic connections than the PAG-to- intermediolateral cell column pathway. If downstream synapses in the descending sensory inhibitory pathway have a greater dependence on endocannabinoid signaling than sympathetic circuits, the former would be slower because the CB1R is a GPCR rather than a ligand-gated ion channel and AEA is believed to be synthesized on demand rather than released from stored vesicles (Felder et al., 1992; Freund et al., 2003; Hansen et al., 1995; Simon and Cravatt, 2008; Ueda et al., 2010).

The data presented here add further evidence supporting cannabinoids as a potentially viable adjunct to multimodal regimens to treat pain conditions. While there is a plethora of basic science literature along with numerous case reports and observational datasets suggesting that cannabinoids are analgesic in humans (Benedict et al., 2022; Habib et al., 2019; Kasai et al., 2022), that evidence has not achieved translation into clinical trials that reach the same conclusion (Nielsen et al., 2022). This is in part due to an incomplete understanding of the cannabinoid-dependent sensory signaling pathways that mediate analgesia. Our new findings suggest that components of endocannabinoid signaling could be promising targets amendable to manipulation by molecular therapy using RNA interference gene knockdown or interfering peptide aptamers for future developments related to analgesia (Xiang et al., 2017).

CRediT authorship contribution statement

Christopher J. Roberts: Conceptualization, Methodology, Formal analysis, Investigation, Visualization, Writing – original draft, Writing – review & editing. **Francis A. Hopp:** Conceptualization, Methodology, Software, Formal analysis, Data curation, Writing – review & editing, Visualization. **Quinn H. Hogan:** Conceptualization, Methodology, Writing – review & editing, Funding acquisition. **Caron Dean:** Conceptualization, Methodology, Software, Formal analysis, Investigation, Writing – original draft, Writing – review & editing, Visualization, Supervision, Funding acquisition.

Declaration of Competing Interest

The authors declare that they have no known competing financial interests or personal relationships that could have appeared to influence the work reported in this paper.

Acknowledgements

The authors would like to thank Victoria Woyach and Claudia Hermes for their excellent technical expertise, as well as Cecilia J. Hillard, Ph.D. and Jeanne L. Seagard, Ph.D. for their invaluable input on experimental design and manuscript preparation. We also thank Margaret Beatka for her artwork in the design of Fig. 9. This work was supported by Merit Review Award # BX001863 from the U.S. Department of Veterans Affairs Biomedical Laboratory Research and Development Program (QHH) and partially supported by T32 GM089586 (CJR) and Career Development Award Number IK2 BX005600 (CJR). The contents do not represent the views of the U.S. Department of Veterans Affairs, the National Institutes of Health, or the United States government.

References

Bago, M., Dean, C., 2001. Sympathoinhibition from ventrolateral periaqueductal gray mediated by 5-HT(1A) receptors in the RVLM. Am. J. Physiol. Regul. Integr. Comp. Physiol. 280 (4), R976–R984.
Bandler, R., Shipley, M.T., 1994. Columnar organization in the midbrain periaqueductal gray: modules for emotional expression? Trends Neurosci. 17 (9), 379–389.
Behbehani, M.M., 1995. Functional characteristics of the midbrain periaqueductal gray. Prog. Neurobiol. 46 (6), 575–605.
Beitz, A.J., 1985. The midbrain periaqueductal gray in the rat. I. Nuclear volume, cell number, density, orientation, and regional subdivisions. J. Comp. Neurol. 237 (4), 445–459.
Benedict, G., Sabbagh, A., Conermann, T., 2022. Medical cannabis used as an alternative treatment for chronic pain demonstrates reduction in chronic opioid use - A prospective study. Pain Physician 25 (1), E113–E119.
Blankman, J.L., Simon, G.M., Cravatt, B.F., 2007. A comprehensive profile of brain enzymes that hydrolyze the endocannabinoid 2-arachidonylglycerol. Chem. Biol. 14, 299–315.
Cameron, A.A., Khan, I.A., Westlund, K.N., Willis, W.D., 1995. The efferent projections of the periaqueductal gray in the rat: a Phaseolus vulgaris-leucoagglutinin study. II. Descending projections. J Comp Neurol 351 (4), 585–601.
Carrive, P., 1993. The periaqueductal gray and defensive behavior: functional representation and neuronal organization. Behav. Brain Res. 58 (1–2), 27–47.
Cravatt, B.F., Giang, D.K., Mayfield, S.P., Boger, D.L., Lerner, R.A., Gilula, N.B., 1996. Molecular characterization of an enzyme that degrades neuromodulatory fatty-acid amides. Nature 384 (6604), 83–87.
Cui, M., Feng, Y., McAdoo, D.J., Willis, W.D., 1999. Periaqueductal gray stimulation-induced inhibition of nociceptive dorsal horn neurons in rats is associated with the release of norepinephrine, serotonin, and amino acids. J. Pharmacol. Exp. Ther. 289 (2), 868–876.
Dampney, R.A., 2015. Central mechanisms regulating coordinated cardiovascular and respiratory function during stress and arousal. Am. J. Physiol. Regul. Integr. Comp. Physiol. 309 (5), R429–R443.
Dean, C., 2011a. Endocannabinoid modulation of sympathetic and cardiovascular responses to acute stress in the periaqueductal gray of the rat. Am. J. Physiol. Regul. Integr. Comp. Physiol. 300 (3), R771–R779.
Dean, C., 2011b. Cannabinoid and GABA modulation of sympathetic nerve activity and blood pressure in the dorsal periaqueductal gray of the rat. Am. J. Physiol. Regul. Integr. Comp. Physiol. 301 (6), R1765–R1772.
Dean, C., Coote, J.H., 1986. Discharge patterns in postganglionic neurones to skeletal muscle and kidney during activation of the hypothalamic and midbrain defence areas in the cat. Brain Res. 377, 271–278.
Dean, C., Hillard, CJ, Seagard, JL, Hopp, FA, Hogan, QH, 2017. Upregulation of fatty acide amide hydrolase in the dorsal periaqueductal gray is associated with neuropathic pain and reduced heart rate in rats. Am. J. Physiol. Regul. Integr. Comp. Physiol. 512 (4), R585–R596.
Egertová, M., Giang, DK, Cravatt, BF, Elphick, MR, 1998. A new perspective on cannabinoid signalling: complementary localization of fatty acid amide hydrolase and the CB1 receptor in rat brain. Proc. Biol. Sci. 265 (1410), 2081–2085.
Farkas, E., Jansen, A.S., Loewy, A.D., 1998. Periaqueductal gray matter input to cardiac-related sympathetic premotor neurons. Brain Res. 792 (2), 179–192.
Felder, C.C., Veluz, JS, Williams, HL, Briley, EM, Matsuda, LA, 1992. Cannabinoid agonists stimulate both receptor- and non-receptor-mediated signal transduction pathways in cells transfected with and expressing cannabinoid receptor clones. Mol. Pharmacol. 42 (5), 838–845.
Finn, D.P., Jhaveri, M.D., Beckett, S.R.G., Roe, C.H., Kendall, D.A., Marsden, C.A., Chapman, V., 2003. Effects of direct periaqueductal grey administration of a

cannabinoid receptor agonist on nociceptive and aversive responses in rats. Neuropharmacology 45 (5), 594–604.
Fox, A., Kesingland, A., Gentry, C., McNair, K., Patel, S., Urban, L., James, I., 2001. The role of central and peripheral Cannabinoid 1 receptors in the antihyperalgesic activity of cannabinoids in a model of neuropathic pain. Pain 92 (1), 91–100.
Freund, T.F., Katona, I., Piomelli, D., 2003. Role of endogenous cannabinoids in synaptic signaling. Physiol. Rev. 83 (3), 1017–1066.
Godlewski, G., Offertáler, L., Wagner, J.A., Kunos, G., 2009. Receptors for acylethanolamides-GPR55 and GPR119. Prostaglandins Other Lipid Mediat. 89 (3-4), 105–111.
Green, A.L., Wang, S., Owen, S.L.F., Xie, K., Bittar, R.G., Stein, J.F., Paterson, D.J., Aziz, T.Z., 2006. Stimulating the human midbrain to reveal the link between pain and blood pressure. Pain 124 (3), 349–359.
Habib, A.M., Okorokov, AL, Hill, MN, Bras, JT, Lee, MC, Li, S, Gossage, SJ, van Drimmelen, M, Morena, M, Houlden, H, Ramirez, JD, Bennett, DLH, Srivastava, D, Cox, JJ, 2019. Microdeletion in a FAAH pseudogene identified in a patient with high anandamide concentrations and pain insensitivity. Br. J. Anaesth. 123 (2), e249–e253.
Hansen, H.S., Lauritzen, L, Strand, AM, Moesgaard, B, Frandsen, A, 1995. Glutamate stimulates the formation of N-acylphosphatidylethanolamine and N-acylethanolamine in cortical neurons in culture. Biochim. Biophys. Acta 1258 (3), 303–308.
Heinricher, M.M., Tavares, I., Leith, J.L., Lumb, B.M., 2009. Descending control of nociception: Specificity, recruitment and plasticity. Brain Res. Rev. 60 (1), 214–225.
Herkenham, M., Lynn, A.B., Johnson, M.R., Melvin, L.S., de Costa, B.R., Rice, K.C., 1991. Characterization and localization of cannabinoid receptors in rat brain: a quantitative in vitro autoradiographic study. J. Neurosci. 11 (2), 563–583.
Hohmann, A.G., Martin, W.J., Tsou, K., Walker, J.M., 1995. Inhibition of noxious stimulus-evoked activity of spinal cord dorsal horn neurons by the cannabinoid WIN 55,212–2. Life Sci. 56 (23-24), 2111–2118.
Hohmann, A.G., Tsou, K., Walker, J.M., 1999. Cannabinoid suppression of noxious heat-evoked activity in wide dynamic range neurons in the lumbar dorsal horn of the rat. J. Neurophysiol. 81 (2), 575–583.
Hohmann, A.G., Suplita, R.L., Bolton, N.M., Neely, M.H., Fegley, D., Mangieri, R., Krey, J.F., Michael Walker, J., Holmes, P.V., Crystal, J.D., Duranti, A., Tontini, A., Mor, M., Tarzia, G., Piomelli, D., 2005. An endocannabinoid mechanism for stress-induced analgesia. Nature 435 (7045), 1108–1112.
Kasai, S., Nishizawa, D, Hasegawa, J, Fukuda, KI, Ichinohe, T, Nagashima, M, Hayashida, M, Ikeda, K, 2022. Short tandem repeat variation in the CNR1 gene associated with analgesic requirements of opioids in postoperative pain management. Front. Genet. 13, 815089.
Keay, K.A., Bandler, R., 2001. Parallel circuits mediating distinct emotional coping reactions to different types of stress. Neurosci. Biobehav. Rev. 25 (7–8), 669–678.
Keay, K.A., Feil, K., Gordon, B.D., Herbert, H., Bandler, R., 1997. Spinal afferents to functionally distinct periaqueductal gray columns in the rat: an anterograde and retrograde tracing study. J. Comp. Neurol. 385 (2), 207–229.
Lau, B.K., Drew, G.M., Mitchell, V.A., Vaughan, C.W., 2014. Endocannabinoid modulation by FAAH and monoacylglycerol lipase within the analgesic circuitry of the periaqueductal grey. Br. J. Pharmacol. 171 (23), 5225–5236.
Lisboa, S.F., Guimaraes, F.S., 2012. Differential role of CB1 and TRPV1 receptors on anandamide modulation of defensive responses induced by nitric oxide in the dorsolateral periaqueductal gray. Neuropharmacology 62 (8), 2455–2462.
Lovick, T.A, 1990. Selective modulation of the cardiovascular response but not the antinocicieption evoked from the dorsal PAG, by 5-HT in the ventrolateral medulla. Pflugers Arch. 416, 222–224.
Lovick, T.A., 1993. The periaqueductal gray-rostral medulla connection in the defence reaction: efferent pathways and descending control mechanisms. Behav. Brain Res. 58 (1–2), 19–25.
Mailleux, P., Vanderhaeghen, J.J., 1992. Distribution of neuronal cannabinoid receptor in the adult rat brain: a comparative receptor binding radioautography and in situ hybridization histochemistry. Neuroscience 48 (3), 655–668.
Maione, S., Bisogno, T., de Novellis, V., Palazzo, E., Cristino, L., Valenti, M., Petrosino, S., Guglielmotti, V., Rossi, F., Marzo, V.D., 2006. Elevation of endocannabinoid levels in the ventrolateral periaqueductal grey through inhibition of fatty acid amide hydrolase affects descending nociceptive pathways via both cannabinoid receptor type 1 and transient receptor potential vanilloid type-1 receptors. J. Pharmacol. Exp. Ther. 316 (3), 969–982.
Mantyh, P.W., 1982a. The ascending input to the midbrain periaqueductal gray of the primate. J. Comp. Neurol. 211 (1), 50–64.
Mantyh, P.W., 1982b. The midbrain periaqueductal gray in the rat, cat, and monkey: a Nissl, Weil, and Golgi analysis. J. Comp. Neurol. 204 (4), 349–363.
Mantyh, P.W., 1983. Connections of midbrain periaqueductal gray in the monkey. II. Descending efferent projections. J. Neurophysiol. 49 (3), 582–594.
Mantyh, P.W., Peschanski, M., 1982. Spinal projections from the periaqueductal grey and dorsal raphe in the rat, cat and monkey. Neuroscience 7 (11), 2769–2776.
Martin, W.J., Patrick, S.L., Coffin, P.O., Tsou, K., Walker, J.M., 1995. An examination of the central sites of action of cannabinoid-induced antinociception in the rat. Life Sci. 56 (23-24), 2103–2109.
Martin, W.J., Hohmann, A.G., Walker, J.M., 1996. Suppression of noxious stimulus-evoked activity in the ventral posterolateral nucleus of the thalamus by a cannabinoid agonist: correlation between electrophysiological and antinociceptive effects. J. Neurosci. 16 (20), 6601–6611.
Menetrey, D., Giesler Jr., G.J., Besson, J.M., 1977. An analysis of response properties of spinal cord dorsal horn neurones to nonnoxious and noxious stimuli in the spinal rat. Exp. Brain Res. 27 (1), 15–33.
Millan, M.J., 2002. Descending control of pain. Prog. Neurobiol. 66 (6), 355–474.
Nielsen, S., Picco, L, Murnion, B, Winters, B, Matheson, J, Graham, M, Campbell, G, Parvaresh, L, Khor, KE, Betz-Stablein, B, Farrell, M, Lintzeris, N, Le Foll, B, 2022. Opioid-sparing effect of cannabinoids for analgesia: an updated systematic review and meta-analysis of preclinical and clinical studies. Neuropsychopharmacology 47 (7), 1315–1330.
Okine, B.N., Gaspar, J.C., Finn, D.P., 2019. PPARs and pain. Br. J. Pharmacol. 176 (10), 1421–1442.
O'Sullivan, S.E., 2007. Cannabinoids go nuclear: evidence for activation of peroxisome proliferator-activated receptors. Br. J. Pharmacol. 152 (5), 576–582.
Palazzo, E., de Novellis, V., Marabese, I., Cuomo, D., Rossi, F., Berrino, L., Rossi, F., Maione, S., 2002. Interaction between vanilloid and glutamate receptors in the central modulation of nociception. Eur. J. Pharmacol. 439 (1-3), 69–75.
Peng, Y.B., Lin, Q., Willis, W.D., 1996a. Effects of GABA and glycine receptor antagonists on the activity and PAG-induced inhibition of rat dorsal horn neurons. Brain Res. 736 (1–2), 189–201.
Peng, Y.B., Lin, Q., Willis, W.D., 1996b. Involvement of alpha-2 adrenoceptors in the periaqueductal gray-induced inhibition of dorsal horn cell activity in rats. J. Pharmacol. Exp. Ther. 278 (1), 125–135.
Peng, Y.B., Lin, Q., Willis, W.D., 1996c. The role of 5-HT3 receptors in periaqueductal gray-induced inhibition of nociceptive dorsal horn neurons in rats. J. Pharmacol. Exp. Ther. 276 (1), 116–124.
Pertwee, R.G., 2005. Pharmacological actions of cannabinoids. In: Pertwee, R.G. (Ed.), Handbook of Experimental PharmacologyCannabinoids. Springer-Verlag, Berlin/Heidelberg, pp. 1–51.
Petrosino, S., Palazzo, E., de Novellis, V., Bisogno, T., Rossi, F., Maione, S., Di Marzo, V., 2007. Changes in spinal and supraspinal endocannabinoid levels in neuropathic rats. Neuropharm. 52 (2), 415–422.
Robinson, C.R., Zhang, H., Dougherty, P.M., 2014. Altered discharges of spinal neurons parallel the behavioral phenotype shown by rats with bortezomib related chemotherapy induced peripheral neuropathy. Brain Res. 1574, 6–13.
Ross, R.A., 2003. Anandamide and vanilloid TRPV1 receptors. Br. J. Pharmacol. 140 (5), 790–801.
Samineni, V.K., Grajales-Reyes, JG, Copits, BA, O'Brien, DE, Trigg, SL, Gomez, AM, Bruchas, MR, Gereau, RW 4th, 2017. Divergent modulation of nociception by glutamatergic and GABAergic neuronal subpopulations in the periaqueductal gray. eNeuro 4 (2) p. ENEURO.0129-16.
Samineni, V.K., Grajales-Reyes, J.G., Sundaram, S.S., Yoo, J.J., Gereau, R.W., 2019. Cell type-specific modulation of sensory and affective components of itch in the periaqueductal gray. Nat. Commun. 10 (1).
Shiosaka, S., Yoshida, S., 2000. Synaptic microenvironments–structural plasticity, adhesion molecules, proteases and their inhibitors. Neurosci. Res. 37 (2), 85–89.
Simon, G.M., Cravatt, B.F., 2008. Anandamide biosynthesis catalyzed by the phosphodiesterase GDE1 and detection of glycerophospho-N-acyl ethanolamine precursors in mouse brain. J. Biol. Chem. 283 (14), 9341–9349.
Starowicz, K., Finn, D.P., 2017. Cannabinoids and Pain: Sites and Mechanisms of Action. Adv. Pharmacol. 80, 437–475.
Tsou, K., Nogueron, M.I., Muthian, S., Sañudo-Peña, M.C., Hillard, C.J., Deutsch, D.G., Walker, J.M., 1998. Fatty acid amide hydrolase is located preferentially in large neurons in the rat central nervous system as revealed by immunohistochemistry. Neurosci. Lett. 254 (3), 137–140.
Tsou, K., Brown, S., Sañudo-Peña, M.C., Mackie, K., Walker, J.M., 1998. Immunohistochemical distribution of cannabinoid CB1 receptors in the rat central nervous system. Neuroscience 83 (2), 393–411.
Ueda, N., Tsuboi, K., Uyama, T., 2010. N-acylethanolamine metabolism with special reference to N-acylethanolamine-hydrolyzing acid amidase (NAAA). Prog. Lipid Res. 49 (4), 299–315.
Walker, J.M., Huang, S.M., Strangman, N.M., Tsou, K., Sañudo-Peña, M.C., 1999. Pain Modulation by Release of the endogenous cannabinoid anandamide. PNAS 96 (21), 12198–12203.
Waters, A.J., Lumb, B.M., 1997. Inhibitory effects evoked from both the lateral and ventrolateral periaqueductal grey are selective for the nociceptive responses of rat dorsal horn neurones. Brain Res. 752 (1–2), 239–249.
Xiang, H., Liu, Z, Wang, F, Xu, H, Roberts, C, Fischer, G, Stucky, C, Dean, C, Pan, B, Hogan, Q, Yu, H, 2017. Primary sensory neuron-specific interference of TRPV1 signaling by AAV-encoded TRPV1 peptide aptamer attenuates neuropathic pain. Mol. Pain 13, p. 1744806917717040.
Xing, J., Li, J., 2007. TRPV1 receptor mediates glutamatergic synaptic input to dorsolateral periaqueductal gray (dl-PAG) neurons. J. Neurophysiol. 97 (1), 503–511.